Variability of Furrow Infiltration and Estimated Infiltration Parameters in a Macroporous Soil

Daniela P. Guzmán-Rojo[1]; Eduardo Bautista, Ph.D., M.ASCE[2]; Julián Gonzalez-Trinidad, Ph.D.[3]; and Kevin F. Bronson, Ph.D.[4]

Abstract: Understanding the spatial and temporal variations of infiltration in furrows is essential for the design and management of furrow irrigation systems. A key difficulty in quantifying the process is that infiltration depends on the depth of flow, which varies along a furrow and with time. An additional difficulty is that under many field conditions, a large fraction of the infiltrated water flows through cracks and/or macropores. This study examines the spatial and temporal variability of a furrow-irrigated field and evaluates a proposed semiphysical furrow infiltration model that accounts for flow-depth and macroporosity effects. Parameter estimation techniques were used to determine two parameters of the infiltration model, the hydraulic conductivity and the macroporosity term, in addition to the Manning roughness coefficient. The methodology was tested using published data from 30 furrow irrigation data sets collected in six furrows over five irrigation events. The evaluation revealed substantial variations in the final infiltrated volume among furrows and from one irrigation event to the next. Variability patterns differed markedly for infiltration measured during the advance phase in comparison with infiltration measured during the storage phase of the irrigations. Advance-phase infiltration varied systematically between irrigations for all furrows. Interfurrow inflow rate variability contributed to the variability of the infiltration during the postadvance phase, but not during the advance phase. Thus, cracks and/or macropores were an important contributor to the variability of infiltration during the advance phase. The analysis produced reasonable estimates of hydraulic conductivity relative to values reported in the literature. Hydraulic conductivity and post-advance infiltration volumes exhibited similar patterns of temporal variability. Hydraulic conductivity estimates were statistically correlated to the applied inflow rate. Although the reasons for this correlation are not clear, a possible explanation is that they are the result of systematic differences in the applied inflow rate among furrows. As with the advance-phase infiltration volumes, the estimated macroporosity term exhibited greater variation among irrigation events than among furrows during an event. The estimation procedure produced smaller differences between volume balance computed infiltration volumes and predicted values when using the semiphysical infiltration model than when using an empirical infiltration equation. Overall, the results show that the proposed furrow infiltration model represents the infiltration process adequately and that, at least for the studied data sets, the proposed estimation procedure yields a coherent set of infiltration and hydraulic resistance parameter values. **DOI: 10.1061/(ASCE)IR.1943-4774.0001366.**

Introduction

The variability of infiltration in space and/or time has been the subject of numerous investigations. Jaynes and Hunsaker (1989), and Childs et al. (1993) among others, showed that irrigated fields can exhibit patterns of spatial variation that are relatively stable with time due to the dominant role of soil texture. Temporal variations can be accounted for, in part, by differences in average antecedent water content and, thus, differences in the soil water pressure gradient, from one irrigation event to the next (Hunsaker et al. 1991). In soils with relatively high clay content, the antecedent water content also affects the development of cracks and macropores (Enciso-Medina et al. 1998). Flow through these pathways dominates infiltration at short opportunity times and can account for two-thirds of the total infiltration volume under typical irrigation conditions (Mitchell and van Genuchten 1993). Cracks and macropores are key contributors to the variability of measured infiltrated volumes over an irrigated field, but quantifying their contribution is difficult, because the scale at which the process takes place is difficult to define. As a result, different measures of variability can be developed depending on the measurement technique or the measurement scale (Bautista and Wallender 1985; Tarboton and Wallender 1989; Hanson et al. 1998). Various concepts have been proposed to model macropore flow (Enciso-Medina et al. 1998; Ahuja et al. 1993; Šimůnek et al. 2003), but their use remains limited for practical irrigation analyses.

In the case of furrow irrigation systems, hydraulic factors—namely, the combined effects of inflow rate, furrow cross-sectional geometry, and hydraulic resistance—also contribute to the variability of infiltration. These variables determine the wetted perimeter, that is, the length of the soil–water interface through which water infiltrates. Some studies have found that average infiltration rate varies proportionally to the wetted perimeter (Fangmeier and Ramsey 1978), which is consistent with infiltration theory. However, other studies have not been able to correlate wetted perimeter with infiltration variation or have measured only a weak

[1]Formerly, Master of Science Student, Dept. of Applied Engineering and Water Resources, Universidad Autónoma de Zacatecas, Zacatecas, ZAC 98000, Mexico. Email: Daniela.guzman.rojo@gmail.com

[2]Research Hydraulic Engineer, US Arid Land Agricultural Research Center, 21881 N. Cardon Lane, Maricopa, AZ 85138 (corresponding author). Email: Eduardo.Bautista@ars.usda.gov

[3]Professor, Dept. of Applied Engineering and Water Resources, Universidad Autónoma de Zacatecas, 801 Ave., Ramón López Velarde, Zacatecas, ZAC 98000, Mexico. Email: aguabuena_62@yahoo.com.mx

[4]Supervisory Soil Scientist, US Arid Land Agricultural Research Center, 21881 N. Cardon Lane, Maricopa, AZ 85138. Email: Kevin.Bronson@ars.usda.gov

Note. This manuscript was submitted on October 2, 2017; approved on August 15, 2018; published online on December 5, 2018. Discussion period open until May 5, 2019; separate discussions must be submitted for individual papers. This paper is part of the ***Journal of Irrigation and Drainage Engineering***, © ASCE, ISSN 0733-9437.

correlation. Several factors may mask the role of hydraulic factors on infiltration variability. One factor is variations in soil texture and structure (Izadi and Wallender 1985; Trout 1992a; Oyonarte et al. 2002). Another factor is the reduction in infiltration rates caused by large flow velocities, which offset the increases in wetted perimeter with inflow (Trout 1992b). Irrigation-induced variations in cross-sectional geometry and hydraulic resistance have also been suggested to offset the effect of variable wetted perimeter along the furrow (Walker and Kasilingam 2004). Finally, some authors have noted that irrigation-induced erosion and deposition alter the hydraulic characteristics of the infiltrating layer (Trout 1992b).

The objective in quantifying infiltration variability is, ultimately, to develop information that can be used for hydraulic analyses of irrigation systems. That information is summarized in the form of infiltration functions—mathematical expressions of the process based on a user-selected equation and calibrated parameters. Empirical equations are most commonly used to model furrow infiltration. These equations express infiltration only as a function of opportunity time. The calibrated parameters are representative of the conditions under which they were calibrated, including the effects of initial and boundary conditions and any other factors that may induce variations in infiltration. As a result, they are difficult to interpret and extrapolate. Nevertheless, various authors have expressed the variability of furrow infiltration in terms of the variability of the parameters of empirical functions (Oyonarte et al. 2002; Khatri and Smith 2006; Gillies et al. 2011).

Furrow infiltration models derived from porous media flow theory potentially offer a more rational approach for studying infiltration variability because they account for hydraulic properties related to soil texture and for initial and boundary conditions (i.e., wetted perimeter effects). While several authors have modeled furrow irrigation flows by coupling the equations of unsteady open-channel flow to the two-dimensional Richards equation (e.g., Wöhling and Schmitz 2007; Banti et al. 2011), those models are difficult to use because of their computational complexity. Semiphysical models currently represent a more promising approach for modeling infiltration in practical furrow irrigation models (Fonteh and Podmore 1993; Enciso-Medina et al. 1998; Warrick et al. 2007; Bautista et al. 2016), because the computations are simpler and because fewer soil parameters need to be determined.

A semiphysical furrow infiltration model (Bautista et al. 2016) was added to WinSRFR (Bautista et al. 2009), a software package for the hydraulic analysis of irrigation systems. Testing of this infiltration model with field data is still limited. A significant challenge for using the model for practical studies is determining the relevant soil parameters. Procedures for the estimation of these parameters from irrigation evaluation data were recently developed (Bautista and Schlegel 2017a, b). In contrast with estimation procedures for empirical furrow infiltration models, estimation procedures for the semi-physical model need to account for the spatial and temporal variation of flow depths. Initial testing of the estimation procedures produced reasonable results. The semi-physical infiltration functions reproduced the observed irrigation flow measurements with, at least, comparable accuracy to empirical infiltration functions. Additional testing is needed to better understand the strengths and limitations of the semiphysical furrow infiltration model and of the proposed procedures for estimating its parameters.

This study examines the spatial and temporal variability of furrow infiltration using a semiphysical infiltration model and parameter estimation methods. Specific objectives are:

- to examine the temporal and spatial variation of infiltration at the scale of irrigated furrows based on irrigation evaluation data and to examine factors that contribute to the spatial and temporal variation of the infiltration;
- to evaluate the ability of the proposed model to represent the infiltration process in a macroporous soil; and
- to characterize the temporal and spatial variation of infiltration and hydraulic resistance parameters estimated from irrigation evaluation data.

Materials and Methods

Field Evaluation Data

Elliott (R. L. Elliott, "Furrow irrigation field evaluation data. Summers of 1977–1979," unpublished report) compiled irrigation evaluation data collected by Colorado State University researchers from several farms. The Benson farm data set, consisting of 30 free-draining furrow evaluations, was selected for this analysis. The evaluations were conducted during five irrigation events at approximately 10-day intervals. During each irrigation, six furrows were evaluated. The furrows were divided into two groups with slightly different soil texture, varying from clay to clay loam. The same furrows were evaluated during each irrigation. In the Elliott report, the furrows are identified by farm (Benson), irrigation number (1–5), group number (1–2), and furrow number (1, 3, and 5) (i.e., 1_2_3 refers to irrigation event 1, group 2, and furrow number 3).

All furrows in the Benson data set have the same average slope S_0 (0.0044) and field length L_f (625 m). Both inflow and outflow rates were measured until near cutoff time t_{co} (the time when inflow to the field was shut off). Advance and recession times were measured every 25 m, but recession was not measured to the end of the field. Flow depths were measured every 50 m, but at most at three times. Every other furrow was irrigated and thus, the reported furrow spacing (FS) was 1.52 m. Extensive cross-sectional data were obtained for these furrows before and after each irrigation, which were used to derive average cross-sectional parameters for each furrow. The data were fitted to a trapezoid and similar parameters were derived for all furrows. A sensitivity analysis showed that volume balance and parameter estimation results, described subsequently, were not very sensitive to the furrow cross-section data, within the range of measured values. Other data included soil texture, bulk density, and gravimetric soil water content before and after the test. The soil water content data were obtained for a single furrow within a group.

Infiltration Analysis and Parameter Estimation

The analysis was conducted using a prerelease version of the WinSRFR 5.0 EVALUE parameter estimation component (Bautista and Schlegel 2017a). EVALUE uses volume balance analysis and unsteady flow simulation to evaluate infiltration and then to estimate the parameters of a selected infiltration model. EVALUE was also used to characterize furrow hydraulic resistance.

In volume balance analyses, infiltrated volume V_z (L^3) is calculated at selected times t_i (T) as the residual of the inflow, surface, and runoff volumes V_{in} (L^3), V_y (L^3), and V_{ro} (L^3), respectively

$$V_z(t_i) = V_{in}(t_i) - V_y(t_i) - V_{ro}(t_i) \tag{1}$$

The values of V_{in} and V_{ro} needed to solve this equation are measured values. For the Benson data set, V_y values were estimated hydraulically as

$$V_y = A_0 \sigma_y x_A \tag{2}$$

where A_0 (L^2) = upstream cross-sectional area, which is a function of the flow-depth y_0 (L); σ_y = dimensionless shape parameter, assumed to vary in the range 0.5–1.0; and x_A (L) = stream length (i.e., the advance distance). Since both the upstream depth y_0 needed to calculate A_0 and σ_y depend on the unknown infiltration function (Bautista et al. 2012), the EVALUE component uses unsteady flow simulation to help refine these estimates (Bautista and Schlegel 2017a).

The times t_i used for the volume balance calculations depend on the available data and the computational strategy used for parameter estimation (Bautista and Schlegel 2017a). The EVALUE component suggests calculation times, which can be modified by the user. For the Benson data set, volume balance can be calculated at the measured advance times and at arbitrary postadvance times up to about 30 min before the reported cutoff time. This was the time at which inflow and/or outflow rate measurements stopped for nearly all furrows.

Infiltration Variability Analysis

This part of the analysis aimed to characterize the spatial and temporal structure of furrow infiltration variability and to identify factors that contribute to that structure. Typically, infiltration variability studies compare volumes determined for a common intake opportunity time (the time that the water is in contact with the soil surface) and under similar hydraulic conditions (length, slope, cross section, inflow rate, resistance). A key difficulty in comparing infiltration volumes measured over entire furrows is that advance times, and therefore opportunity times as a function of distance, may vary substantially among the evaluated furrows. Differences in hydraulic conditions exacerbate differences in opportunity time and, furthermore, create diffierences in the magnitude of the infiltrating surface. This is the case for the Benson data set, for which inflow rates varied systematically among furrows while cutoff times varied from one irrigation event to the next.

Recognizing the dissimilarity of opportunity times and hydraulic conditions for these furrows, infiltration variability was examined from three measurements of infiltration, namely infiltration at the end of the advance phase, infiltration at a common average intake opportunity time, and infiltration determined at the final volume balance calculation time, that is, the maximum time allowed by the data (about 30 min before the reported cutoff time for each furrow, as explained previously). These three measurements are identified subsequently as, respectively, V_{zadv}, V_{ziot}, and V_{zf}. In principle, comparison of infiltration at the end of the advance phase with infiltration at later times should provide measures of the contribution of macropore and porous media flow to total infiltration.

The average intake opportunity time $\mathrm{IOT}_{\mathrm{avg}}$ of a furrow, for times less than the initial recession time, is given by

$$\mathrm{IOT}_{\mathrm{avg}} = \frac{\int_0^{x_A} (t_i - t_{adv}(x))dx}{x_A} \tag{3}$$

where $t_{adv}(x)$ = advance time to distance x; and other variables are as previously defined. For $t_i \geq t_L$ (the final advance time), $x_A = Lf$. An $\mathrm{IOT}_{\mathrm{avg}}$ value was calculated for each furrow, initially with t_i equal to the maximum time at which inflow rate was measured. Trapezoidal rule integration was used to solve Eq. (3) using the field-measured values of $t_{adv}(x)$. The smallest $\mathrm{IOT}_{\mathrm{avg}}$, 367 min, was selected as the common value. For each furrow, t_i was adjusted to force $\mathrm{IOT}_{\mathrm{avg}} = 367$ min. This value of t_i, identified as t_i^*, was used in combination with Eq. (1) to calculate V_{ziot}.

Multivariable regression analyses were conducted to assess the contribution of interfurrow flow rate variability and of the categorical variables furrow group and irrigation number to the variability of the infiltrated volumes V_{zadv}, V_{ziot}, and V_{zf}. Although it would have been desirable to do so, initial water content was not included in the analysis as an independent variable because of the paucity of those data. The contribution of furrow-to-furrow variation was not examined either because, as will be explained subsequently, furrow-to-furrow variation effects are confounded with inflow rate variability. The analysis was conducted with the R version 3.5.0 software package (R Core Team 2017). The analysis first tested the model

$$V_z = Q_{in} + \mathrm{Irr} + \mathrm{Group} + \varepsilon \tag{4}$$

using the R *lm* function. In Eq. (11), V_z stands for either V_{zadv}, V_{ziot}, or V_{zf}, and ε is the random error. Unneeded predictors were then eliminated by testing nested submodels and comparing the nested models with the model defined by Eq. (4) using the *anova* function. Quantile-quantile plots were developed to confirm that the raw data and the residuals of the regression followed a normal distribution (Caffo 2015). Possible interactions were also explored but were not significant. Details of the analyses are provided in Guzmán-Rojo (2017).

Infiltration Model

Warrick et al. (2007) proposed a furrow infiltration model based on an approximate solution to the two-dimensional Richards equation. Following modifications suggested by Bautista et al. (2014), the model can be written as

$$A_z(t) = z(t)\mathrm{WP} + \frac{\gamma S_0^2 t}{\Delta\theta} \tag{5}$$

where A_z = infiltration volume per unit length (L^2); z = one-dimensional infiltration volume per unit area (L); WP = wetted perimeter (L); S_0 = soil sorptivity ($L/T^{0.5}$); $\Delta\theta$ = difference between saturated and initial water content (L^3/L^3); t = time (T); and γ = dimensionless empirical parameter related to boundary conditions, geometry, and initial conditions, typically in the range 0.6–1.0 (Warrick et al. 2007; Bautista et al. 2014). In this model, infiltration is the result of vertical and lateral flow components, represented by, respectively, the first and second terms in the equation. Eq. (5) was developed under the assumption of a constant ponding depth.

Eq. (5), modified to account for the effect of a variable ponding depth (Bautista et al. 2016), was used in this study. The one-dimensional infiltration term z was computed with the Green and Ampt (1911) equation:

$$z = z_0 + K_s(t - t_0) + \Delta\theta\Delta h \cdot \ln\left(\frac{z + \Delta\theta\Delta h}{z_0 + \Delta\theta\Delta h}\right) \tag{6}$$

where z = infiltrated depth (L^3/L^2); z_0 = infiltration at time t_0; Δh = difference between the average water pressure at the infiltrating surface h_{1D} (Bautista et al. 2014) and the wetting front pressure head h_f (a negative value, also referred to as the wetting front capillary suction); K_s = saturated hydraulic conductivity (L/T); and other variables are as previously defined. The Green-Ampt parameters can also be used to estimate S_0 in Eq. (5) (Warrick et al. 2007):

$$S = \sqrt{2K_s\Delta\theta\Delta h} \tag{7}$$

Eqs. (5)–(7) were developed based on porous media flow theory. In practice, large volumes of water can bypass the soil matrix and flow instead through macropores and cracks. Clemmens and Bautista (2009) noted that the Green-Ampt equation often fails

to fit field-measured infiltration data due to the effects of macropore flow. Although several authors have attempted to describe macropore flow using physical principles, Clemmens and Bautista (2009) suggested adding a macropore depth term (volume per unit area) to the Green-Ampt equation, under the assumption that such a volume infiltrates instantaneously. Here, the macropore term is labeled c_{GA}. To use this concept with furrows, we assume that macropore flow does not depend on the wetted perimeter, but rather, on the furrow spacing FS. After adding these terms and expressing S_0 with Eq. (7), Eq. (5) becomes

$$A_z = z \cdot \mathrm{WP} + c_{GA} \cdot \mathrm{FS} + 2\gamma K_s \Delta h \cdot t \tag{8}$$

which depends on the parameters θ_0, θ_s, h_f, K_s, c, and γ. This expression, in combination with Eq. (6), is identified in the following discussion as the Warrick-Green-Ampt (WGA) model.

Estimation of the Flow-Depth Dependent Infiltration Parameters

In EVALUE, infiltration parameters are found by minimizing the objective function

$$\mathrm{OF} = \sum_{i=1}^{I} (V_z - V_z^*)^2 \tag{9}$$

where V_z = volumes calculated with Eq. (1); V_z^* = infiltration volumes calculated by integrating the infiltration profile with a selected infiltration model over the length of the stream at the given time, $x_A(t_i)$; and I = number of times t_i is used for volume balance calculations. For these data sets, the software selected 11 or fewer volume balance calculation times.

In typical applications of the volume balance method, for parameter estimation, infiltration is assumed to depend on opportunity time only. Various procedures are available to calculate V_z^* under such conditions (Strelkoff et al. 2009). In this analysis, Eqs. (8) and (6) depend on the flow depth variation along the field and with time, $y(x, t)$, and on the unknown parameters K_s and c_{GA}, hence

$$V_z^*(t_i) = \int_0^{x_A(t_i)} A_z(y(x,t), K_s, c_{GA})dx \tag{10}$$

EVALUE uses a two-step process for the estimation of flow-depth dependent infiltration parameters (Bautista and Schlegel 2017b). The first step consists of the estimation of an empirical infiltration function, dependent on opportunity time only and, thus, independent of wetted perimeter variations along the furrow and with time. The modified Kostiakov equation was used in this initial stage:

$$A_z = W_1(k\tau^a + b\tau) + W_2 c \tag{11}$$

where k (L/T^a), a, b (L/T), and c (L) are empirical parameters; k and a represent transient infiltration; b = steady infiltration rate; c = instantaneous macropore infiltration, similar to the term c_{GA}; and W_1 and W_2 are transverse widths (L). For these analyses, both W_1 and W_2 were set equal to the furrow spacing FS. Eq. (10) was expressed as a function of the parameters of Eq. (11) and used to solve Eq. (9) based on the available volume balance data. This first step also yielded estimates for the resistance coefficient of the selected hydraulic resistance model, as will be explained subsequently.

In the second step, an unsteady flow simulation was conducted with the estimated empirical infiltration function. This simulation produces the $y(x, t)$ needed to solve Eq. (10), and, subsequently, Eq. (9). This step relies on the nonuniqueness of solutions to the infiltration parameter estimation problem; nearly identical flow depth and flow rate conditions can be simulated with different infiltration functions, as long as the functions predict the same average infiltration (Bautista 2016). This analysis estimated the parameters K_s and c_{GA} from field evaluation data; θ_0 was measured, and θ_s and h_f were estimated from pedotransfer functions. Since γ often is close to unity, its value was assumed to be subsumed in the estimated K_s.

Determination of θ_0, θ_s, and h_f

As was previously indicated, Elliott reported preirrigation gravimetric water content and bulk density data. Those data were measured in one furrow only for each group and at three distances along the furrow. At each location, samples were obtained at five soil depth intervals and at three locations across the furrow spacing. Considering the paucity of the data and the fact that the analysis assumes a uniform soil profile, those data were averaged to determine θ_0 for each group and irrigation event.

Rawls et al. (1983) reported values for parameters of the Green-Ampt equation based on soil texture. The average values reported for a clay loam soil, $\theta_s = 0.45$ and $h_f = -43$ cm, were selected for this study.

Modeling Hydraulic Resistance and Estimation of the Resistance Parameter

The Manning equation is commonly used to model hydraulic resistance in surface irrigation:

$$S_f = \frac{n^2 v|v|}{c_u^2 R^{4/3}} \tag{12}$$

where S_f = friction slope (L/L); v = flow velocity (L/T); R = hydraulic radius (L); c_u = units coefficient (= 1 m$^{0.5}$/s in SI units); and n (L$^{1/6}$) = resistance coefficient.

Estimates of the Manning n were developed with the EVALUE component by fitting the simulated flow depths as a function of distance and time to measured values. Since estimates of V_y with Eq. (2) depend on the roughness parameter, the analysis required first estimating the infiltration function based on an assumed n value. Unsteady simulation was then conducted with that infiltration function and the resulting depths were used to manually adjust n. Goodness-of-fit indicators provided by the software were used to compare simulated with observed values. The adjusted n was used to refine the volume balance computations and estimate a new infiltration function. No further adjustments to n were required after this step, even with further changes to the infiltration parameters. Additional details on the process used to determine n with EVALUE are provided in Bautista and Schlegel (2017b).

Wetted Perimeter Contribution to Infiltration Variability

A premise of this study is that wetted perimeter variability among furrows contributes to the spatial and temporal variability of infiltration. Inflow rate variability is a key factor contributing to wetted perimeter variability. This inflow rate/wetted perimeter effect can be examined with free-draining furrows by comparing the inflow rate with the furrow infiltration rate Q_z, calculated as the difference between the inflow Q_{in} and runoff rates Q_{ro}. In principle, this calculation should be made when the runoff rate is at or near steady-state. For the Benson data set, the calculation was made near cutoff time, depending on the inflow and outflow measurements available for each furrow and was not, in all cases, near steady conditions.

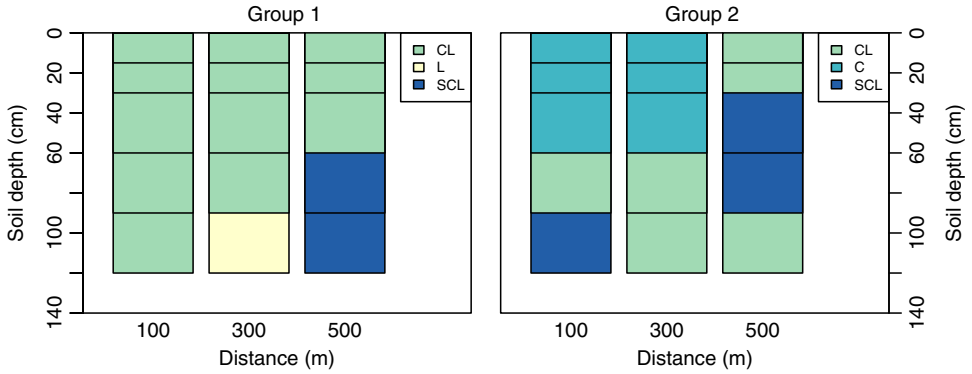

Fig. 1. Textural variation with soil depth for each furrow group.

This field-measured relationship was then compared with a theoretical relationship determined via simulation using the simulation component of WinSRFR. Simulations were conducted with infiltration given by the WGA model and with the K_s and c_{GA} parameters set equal to the mean of the estimated parameters. In these simulations, inflow rates were varied between 1.2 and 2.8 L/s, which is nearly the range of inflows reported for the Benson furrows, and cutoff time was set equal to 600 min, which is approximately the average cutoff time for these evaluations. An average value was also used for the Manning resistance coefficient. The infiltration rate for each furrow was calculated as the difference between the inflow and outflow rates at cutoff time.

Results

Background Information

This section provides background information that is needed to understand the variability of infiltration measurements for the evaluation data set. Fig. 1 summarizes the soil texture information for the Benson furrows. These data were obtained on a single transect for each furrow group. As was noted previously, the soil for furrows in Group 1 was primarily clay loam, while the soil for furrows in Group 2 was mostly a combination of clay loam and clay. While limited, these data suggest fairly uniform soil conditions along each field, and moderate differences between the two furrow groups.

Fig. 2 presents the average inflow rate applied to each furrow during each irrigation. As indicated by the x-axis labels, the furrows are separated by group number (G1 and G2, respectively). Different symbols and lines are used to represent different irrigation events (identified in the graph as Irr1–Irr5). The Elliott report does not explain the criteria used to set the inflow rate for each of the 30 evaluations. However, systematic inflow rate variations are evident from the data. With the exception of the first irrigation, the inflow rate applied to each furrow was nearly the same throughout the irrigation season, but inflow rates differed among furrows. Larger inflow rates were applied to furrows in Group 1 than to those in Group 2. Since cutoff times were nearly the same for all furrows during each irrigation, infiltration variations can be expected among the furrows for each irrigation event and between irrigation events simply due to the differences in the applied volume. In other words, with this data set, soil texture and/or structural effects on infiltration are confounded with the effect of variable inflow rates and applied volume.

Elliott (1980) reported irrigation requirement depths, calculated from weather and crop development data, but did not explain whether irrigation cutoff times were determined based on the irrigation requirements. Fig. 3 displays the irrigation requirement volume (V_{req}) (the product of irrigation requirement depth, furrow length, and spacing) and also summarizes the average application volume (V_{in}) by irrigation. With the exception of the first irrigation, the average applied volume was only slightly greater than required volume, and in the case of Irrigation 5, it was even less. In fact, for all irrigations except the first, the application did not satisfy the reported requirements for one or more furrows, particularly the furrows in Group 2. The significance of these results is that, just as with the variation in applied volume among furrows, there is a variation in applied volume among irrigations that is unrelated to the irrigation requirements. It is likely that cutoff time and

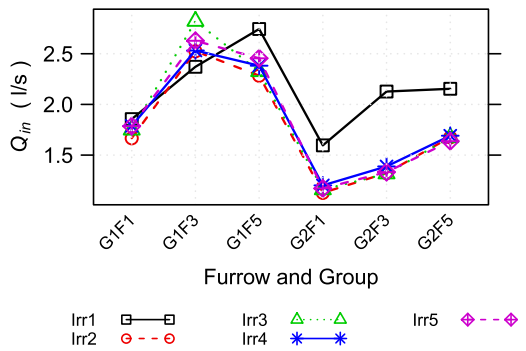

Fig. 2. Applied average inflow rate for each furrow and irrigation. The labels G and F refer to group and furrow numbers, respectively.

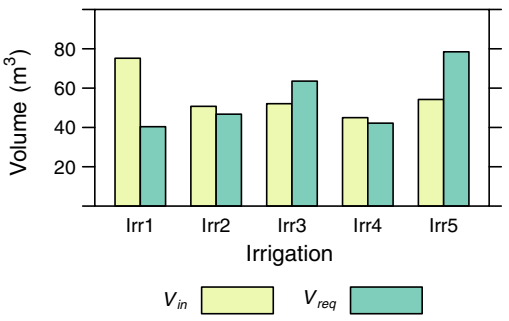

Fig. 3. Average applied and irrigation requirement volumes (V_{in} and V_{req}, respectively) for each irrigation.

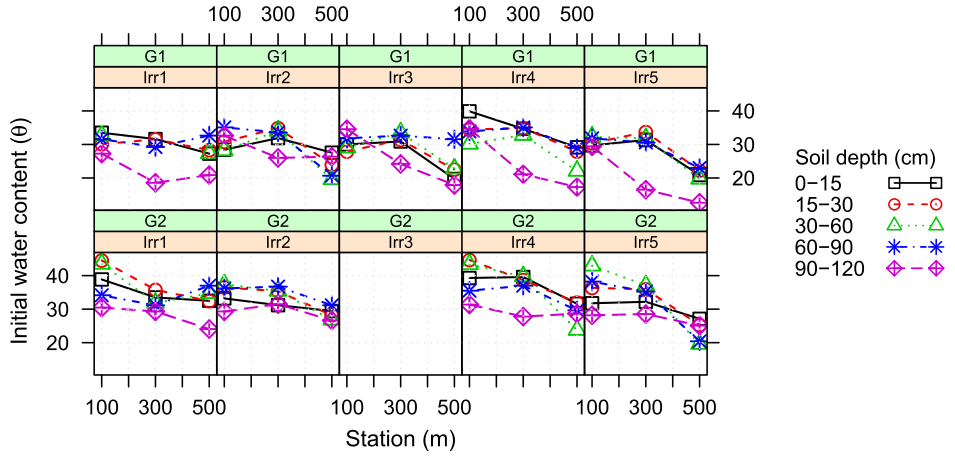

Fig. 4. Variation in the initial volumetric water content with depth for each irrigation and furrow group.

applied water were determined by labor constraints and/or by irrigator experience.

The aforementioned discussion of results implies differences in initial water content among furrows, especially differences between furrows in Groups 1 and 2. The available water content data allows for examination of this issue, but only in a limited way. Water contents were measured in only one furrow per group, different from the furrows where flow variables were measured. Fig. 4 illustrates the preirrigation volumetric soil water content with depth for each irrigation (Irr) and group (G). Each point is the average of measurements obtained at three transverse locations. Except for the lower soil depth, water content appears to have been fairly similar before each irrigation. The decline in water content at the lower depth would appear to confirm that the water applications did not meet the irrigation requirement. Therefore, water was mined from the lower profile. The results also show a declining water content trend with distance, which is consistent with variations in opportunity time with distance typical of surface irrigation systems but could also be related to the presence of sandy clay loam toward the end of both fields (Fig. 1).

Average preirrigation water content for each irrigation and soil group are given in Table 1. These results show that preirrigation water content was, on average, similar for all irrigations, although the average water application amounts (Fig. 3) varied substantially among irrigations. Also, the water content for Group 2 was slightly greater than for Group 1, which is consistent with differences in textural characteristics (Fig. 1), but not consistent with the systematic differences in water application (Fig. 3). Table 1 also displays the interval between irrigations. For purposes of the following discussion, it is important to note that Irrigation 4 had the shortest interval, while Irrigations 3 and 5 had the longest interval. Except for Irrigation 5, the preirrigation water content seems unrelated to the irrigation interval. The relatively low initial water content for irrigation 5 (Table 1) is consistent with a long interval between irrigations and an advanced crop development stage. Since no measurements were obtained for Irrigation 3, Group 2, the initial water content was assumed equal to 0.32 based on the values given in the table for other irrigations in the same group.

Table 1. Intervals between irrigations and average initial volumetric water content for each furrow group and irrigation

		θ_0	
Irrigation number	Irrigation interval (days)	Group 1	Group 2
1	—	0.28	0.33
2	10	0.28	0.32
3	12	0.28	N/A
4	8	0.28	0.32
5	12	0.26	0.29

Variability of Infiltration Determined from Volume Balance

Fig. 5 depicts V_{zadv}, V_{ziot}, and V_{zf} for each furrow, grouped by irrigation event. If infiltration was due only to porous media flow, infiltration variations for the postadvance phase would resemble those observed during the advance phase. Except for Irrigation 1,

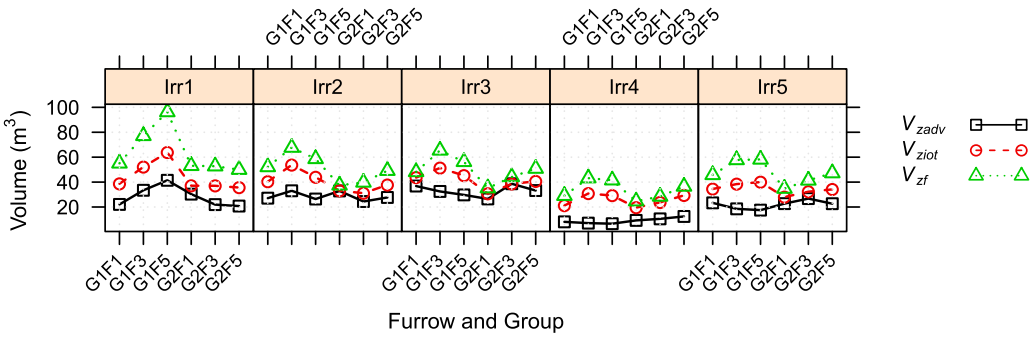

Fig. 5. Infiltration volumes V_{zadv}, V_{ziot}, and V_{zf} for each furrow and irrigation.

Table 2. Statistical summary by irrigation for infiltration and inflow volumes

Infiltration (m^3)	Irrigation 1	2	3	4	5	Avg.
At final advance time (V_{zadv})						
Avg.	28.3	28.6	32.9	9.0	21.9	24.0
COV (%)	29	12	14	24	15	19
At average opportunity time (V_{ziot})						
Avg.	43.0	39.8	41.5	25.3	34.3	36.8
COV (%)	28	20	17	19	13	19
At final volume balance calculation time (V_{zf})						
Avg.	64.0	50.8	50.0	35.6	47.5	49.6
COV (%)	29	23	21	17	19	22
Inflow volume (V_{in})						
Avg.	91.3	64.3	65.9	55.3	67.2	68.8

Note: Avg. = average; and COV = coefficient of variation.

different infiltration patterns were produced by the advance and postadvance phase data. From one irrigation to the next for each furrow, V_{zadv} exhibited substantial variations. Particularly noticeable are the results of Irrigation 4, which produced the smallest V_{zadv} values for all furrows. This large infiltration variation among irrigation events is consistent with the presence of soil macropores and/or cracks. It is likely that those flow conduits did not develop as extensively for Irrigation 4, due to the short irrigation interval (Table 1).

A factor that contributed to differences in the variability patterns for V_{zadv} and V_{ziot} is that the former were calculated for a wide range of IOT_{avg} values while the latter were computed for a single IOT_{avg}. During advance, the mean IOT_{avg} was 151 min, with a CV of 48%, while V_{ziot} values were computed for $IOT_{avg} = 367$ min. In contrast, V_{zf} and V_{ziot} exhibited similar variability patterns, even though the former were computed for IOT_{avg} values ranging from 480 to 627 min (mean = 498 min, CV = 13%). This similar pattern of variation for V_{zf} and V_{ziot} is consistent with porous media flow theory, as it persisted from one irrigation event to the next.

Tables 2 and 3 display the mean and COV computed for the data in Fig. 5, the former by irrigation event and the latter by furrow. The irrigation event–averaged V_{zadv} (Table 2) varied between 9 and nearly 33 m^3, while the furrow-averaged V_{zadv} (Table 3) varied beween about 23 and 25 m^3. In contrast, the COV varied between 12% and 29% for the irrigation event–averaged data but between 33% and 54% for the furrow-averaged values. These results emphasize again the substantial differences in advance-phase infiltration among irrigation events. During the postadvance phase, differences in average infiltration volume increased among furrows (Table 2),

Table 3. Statistical summary by furrow for infiltration volumes

Infiltration (m^3)	Furrow G1F1	G1F3	G1F5	G2F1	G2F3	G2F5	Avg.
At final advance time (V_{zadv})							
Avg.	22.8	24.9	24.3	24.3	24.5	23.3	24.0
COV (%)	45	47	54	38	41	33	43
At average opportunity time (V_{ziot})							
Avg.	35.4	44.9	44.1	29.4	31.4	35.3	36.8
COV (%)	25	22	28	23	17	12	21
At final volume balance calculation time (V_{zf})							
Avg.	46.0	62.2	62.2	39.0	41.3	46.7	49.6
COV (%)	22	20	33	20	21	13	22

Note: Avg. = average; and COV = coefficient of variation.

presumably due to spatial differences in furrow inflow and infiltration rates, while relative differences among irrigations decreased (Table 3). Average V_{zf} values for each irrigation were closely related to the average inflow volume V_{in}. Those values are displayed in the last row of Table 2.

Fig. 6 displays V_{zadv}, V_{ziot}, and V_{zf} as a function of the inflow rate Q_{in}. The data are separated again by irrigation but are also separated by group number. Regression lines through each group of 3 furrows highlight trends in the data. One can expect final advance times to decrease and, consequently, infiltrated volumes to decrease with increasing flow rate during the advance phase. Except for the furrows in Group 2 during the first irrigation, advance times decreased with increasing flow rate, as expected (not illustrated). However, infiltration varied somewhat randomly with inflow rate for these furrows. For the furrows in Group 1, V_{zadv} increased with Q_{in} during the first two irrigations but then decreased during the last three. The furrows in Group 2 exhibited essentially the opposite trend, except for the last irrigation. In contrast, V_{ziot} and V_{zf} increased with Q_{in} (lower plots), and the regression lines exhibited similar slopes, especially during the last three irrigations. Again, macropore flow can help explain why infiltrated volume seems unrelated to Q_{in} during advance. A key reason for the increased postadvance infiltration is that larger inflow rates increased the opportunity times during the storage phase of each irrigation due to the reduced time needed to reach the end of the field. Another potential contributing factor is that the wetted perimeter, and therefore the infiltrating surface, increased with Q_{in}, but this effect cannot be assessed from these data.

Hanson et al. (1998) examined infiltration on the scale of furrows in a cracking clay soil. As with the evaluations reported herein, Hanson et al. (1998) tested different inflow rates on furrows on the same field and conducted evaluations over several irrigations. While they did not examine advance-phase infiltration separately from postadvance infiltration, they found that when cracks were visible, final infiltration was unrelated to the applied inflow rate. When tillage operations removed the cracks, infiltration increased with inflow rate. Hence, the results in Figs. 5 and 6 support those of Hanson et al. (1998).

Results of the multivariable regression analysis for the three infiltration variables are summarized in Tables 4–6. Group number was eliminated as a predictor in all analyses, which, again, may be related to the fact that the applied inflow rate systematically differed beween groups and among furrows within each group. Since the analysis for V_{zadv} also eliminated Q_{in}, the variation of V_{zadv} was explained by irrigation number alone (adjusted $R^2 = 0.74$). Only Irrigation 4 produced a highly significant predictor estimate (Table 4). According to this model, nearly 19 m^3 less water was required to advance to the end of the field during Irrigation 4 than during Irrigation 1, with $Pr < 0.001$. Less volume was also required for the last irrigation, although the difference was much smaller.

In contrast, differences in V_{ziot} (Table 5) and V_{zf} (Table 6) were explained by both Q_{in} and irrigation number (adjusted $R^2 \geq 0.77$). As expected, the predictor estimate for Q_{in} was positive and highly significant ($Pr < 0.001$) in both analyses. As with V_{zadv}, the predictor estimate associated with Irrigation 4 was negative and highly significant. Note, however, that predictor estimates for V_{zf} became either negative or increasingly negative in comparison with those computed for V_{ziot} and that the estimate for Irrigation 3 became statistically significant. This shows that post-advance-phase infiltration, presumably controlled by porous media flow effects, eventually overshadowed advance-phase infiltration variabiilty.

A final issue to examine in this section is the correlation for the different infiltration volumes between consecutive irrigation events

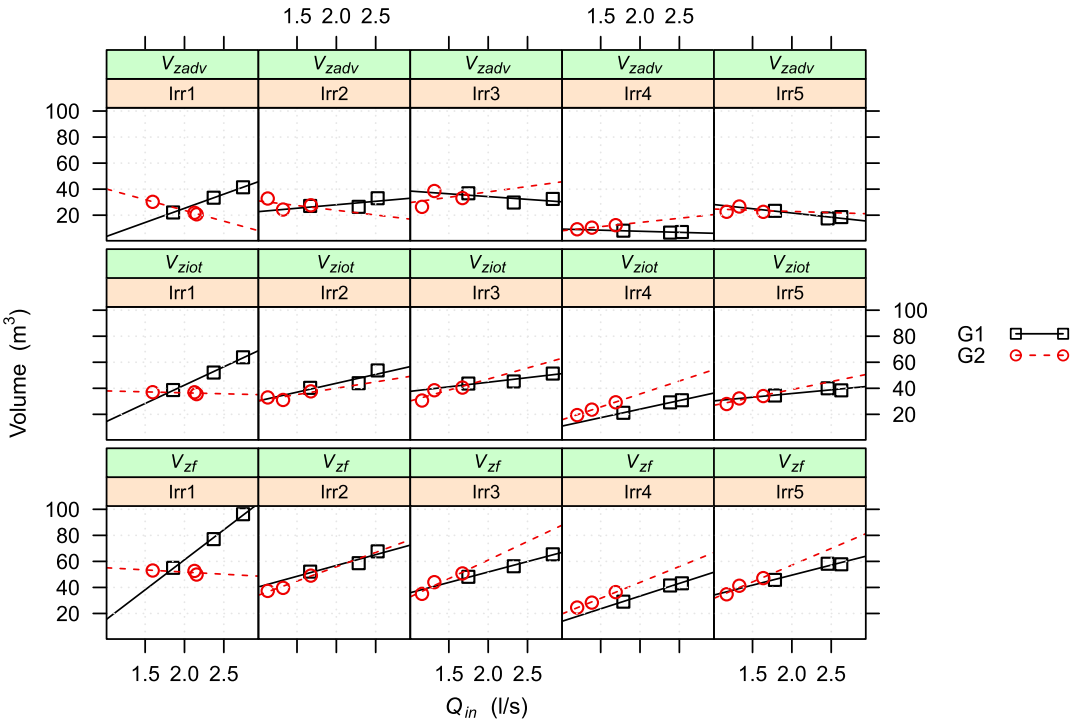

Fig. 6. Infiltration volumes V_{zadv}, V_{ziot}, and V_{zf} as a function of inflow rate.

Table 4. Multiple linear regression results for V_{zadv} (m^3)

Predictor	Estimate	Standard error	Pr (>|t|)
Intercept	28.33	1.97	<0.001[a]
Irr2	0.26	2.79	0.927
Irr3	4.57	2.79	0.114
Irr4	−19.33	2.79	<0.001[a]
Irr5	−6.41	2.79	0.030[b]

Note: Multiple R^2: 0.78; adjusted R^2: 0.75.
[a]Statistical significance: 0.001 level.
[b]Statistical significance: 0.05 level.

Table 5. Multiple linear regression results for V_{ziot} (m^3)

Predictor	Estimate	Standard error	Pr (>|t|)
Intercept	20.19	3	<0.001[a]
Q_{in} (L/s)	11.15	1.71	<0.001[a]
Irr2	0.10	2.76	0.97
Irr3	0.98	2.74	0.72
Irr4	−14.96	2.74	<0.001[a]
Irr5	−6.08	2.74	0.04[b]

Note: Multiple R^2: 0.81; adjusted R^2: 0.77.
[a]Statistical significance: 0.001 level.
[b]Statistical significance: 0.05 level.

Table 6. Multiple linear regression results for V_{zf} (m^3)

Predictor	Estimate	Standard error	Pr (>|t|)
Intercept	24.09	5.90	<0.001[a]
Q_{in} (L/s)	18.66	2.45	<0.001[a]
Irr2	−6.27	3.95	0.13
Irr3	−8.43	3.91	0.04[b]
Irr4	−24.35	3.91	<0.001[a]
Irr5	−10.79	3.91	0.01[b]

Note: Multiple R^2: 0.83; adjusted R^2: 0.80.
[a]Statistical significance: 0.001 level.
[b]Statistical significance: 0.05 level.

Table 7. Pearson correlation for infiltration volumes between consecutive irrigations

Irrigations	V_{zadv}	V_{ziot}	V_{zf}
Irr 1–2	0.31	0.73	0.71
Irr 2–3	−0.66	0.84[a]	0.96[b]
Irr 3–4	0.26	0.75	0.94[b]
Irr 4–5	0.69	0.8	0.96[b]

[a]Statistical significance: 0.05 level.
[b]Statistical significance: 0.01 level.

(Table 7). No correlation was determined for the advance-phase infiltration volumes. Values of V_{ziot} produced larger correlation coefficients, but only Irrigations 2 and 3 produced statistically signfiicant results. Highly significant (Pr < 0.01) correlations were determined for the V_{zf} values between Irrigations 2 and 3, 3 and 4, and 4 and 5. These results support previous studies that showed that well-defined patterns emerged after the first irrigation, likely due to soil consolidation (Childs et al. 1993). Limited cultural practices were reported for the Benson furrows during the irrigation seasons. The results also suggest that similarities in infiltration patterns between consecutive irrigations were due to porous media flow, which, as was previously indicated, overshadowed the advance-phase infiltration. The systematic variation in applied inflow rate could also help explain the strong correlation between consecutive events. Childs et al. (1993) examined infiltration volumes measured in furrow sections and reported that the correlation between

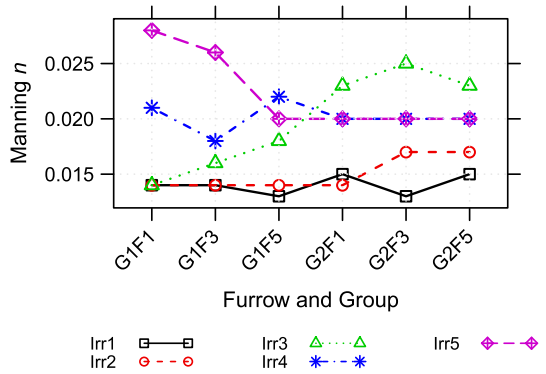

Fig. 7. Estimated Manning n values for each furrow and irrigation.

irrigation events strengthened as the irrigation season evolved. They attributed the changes in correlation to the presence of cracks and cultural practices during earlier irrigations.

Estimated Parameters

The first step of the estimation procedure was the most difficult, because it involved four infiltration parameters and one roughness parameter. The estimated parameters of the modified Kostiakov Eq. (11) are unimportant for purposes of this study, but it is worth noting that k and c were significantly correlated with Vz_{adv} while b was correlated with V_{zf}. Pearson correlation coefficients of, respectively, 0.43, 0.74, and 0.75 were computed for each of these variables. The fitting of the Manning n also merits some comment. The fitting involves comparing predicted and measured depth hydrographs. The difficulty of this approach, at least for this particular data set, is that because the measured flows depths were generally very shallow (generally less than 4 cm deep at the inlet), small measurement errors translate into large data scatter. More data is available for the initial irrigations, and the data collected later exhibits more scatter. As a result, Manning n estimates cannot be considered very precise and variations in these values among furrows are difficult to explain. Still, the results suggest that the furrows were smoother during the earlier irrigations than during the latter irrigations (Fig. 7). Hydraulic resistance can increase during the irrigation season as a result of the accumulation of dry plant material on the soil surface. The computed n values were always less than the value typically recommended for bare furrows ($n = 0.04$).

Fitting the WGA model parameters was easier than the first step of the estimation process, because there were only two parameters to consider. In addition, and more importantly, while matching the predicted infiltrated volumes to the values computed from volume balance data, the effect of each parameter was easily discernible; infiltrated volumes during advance were strongly dependent on the parameter c_{GA}, while postadvance results mostly depended on K_s.

Several metrics are available to assess the goodness-of-fit of the estimated parameters and, consequently, the ability of the WGA equation to represent infiltration under the given field conditions. One metric is the objective function [OF—Eq. (8)], that is, the sums-of-squares resulting from estimation with the modified Kostiakov model compared to values computed with the WGA model. While the OF values were of similar magnitude, smaller values were computed with the latter equation for 29 of the 30 evaluation data sets. Thus, at least for this data set, the WGA equation provided an improvement over the empirical infiltration model. A second metric is the root-mean-square error (RMSE) (the square root of the sums-of-squares divided by the number of observations) expressed as a percent of the applied volume V_{in}. This value was only 1.3% for the event with the largest RMSE, while the average value from all 30 evaluations was 0.5%. These values attest to the quality of the field data. Last, for each test, recession times were measured at a limited number of locations. A comparison of the simulated recession times with the measured values, which were not used for estimation, provided an independent verification of the estimated infiltration and resistance parameters. The RMSE of the recession times was computed for each test using the estimated modified Kostiakov and WGA infiltration functions. On average, those values were 7.8 and 4.7 min, respectively. The improved recession predictions were likely related to the diminishing wetted perimeter during recession, which reduced infiltration and slightly increased recession times.

Fig. 8 displays the estimated infiltration parameters K_s and c_{GA}. Note that the estimated hydraulic conductivities, which range from 0.28–0.98 cm/h, are consistent with values reported in the literature for a clay loam soil (Rawls et al. 1983; Saxton and Rawls 2006). Since macropore flow appears to be substantial for the Benson furrows, and those effects manifest themselves during advance, it is not surprising that the pattern of variation for c_{GA} values exhibited strong similarities to that of $Vz(t_L)$, while the corresponding pattern for the hydraulic conductivity resembled the pattern for $V_{z(sto)}$. Pearson correlation coefficients were computed between K_s and V_{zf} and between c_{GA} and Vz_{adv}. Strong and statistically significant values were computed in both cases—0.92 and 0.86, respectively.

Of note in Fig. 8(a) is the K_s computed for the first irrigation for Furrow 5 in Group 1. This result is consistent with the large $V_{z(sto)}$ computed for the same furrow (Fig. 5). However, the difference between K_s values computed for other irrigations for the same furrow seems proportionally larger than the difference for the $V_{z(sto)}$ values. Thus, this result could be an artifact of the estimation

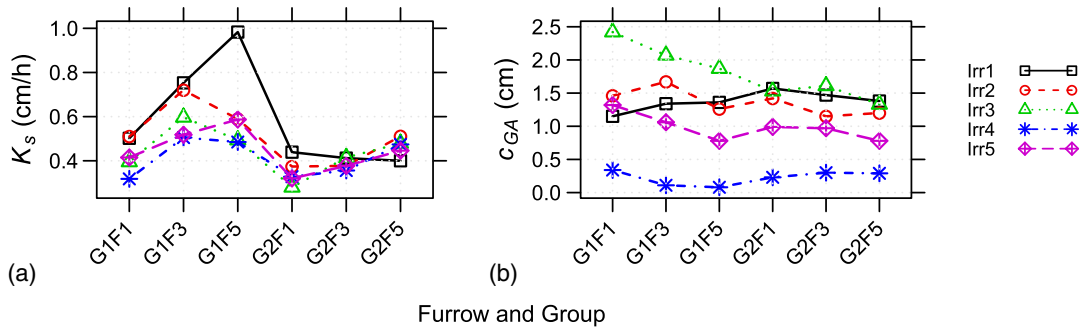

Fig. 8. Estimated: (a) hydraulic conductivity; and (b) macropore constants for each furrow and irrigation.

Table 8. Statistical summary for hydraulic conductivity and macropore constant for each furrow

Group and Furrow	K_s (cm/h)		c_{GA} (cm)	
	Mean	COV (%)	Mean	COV (%)
G1F1	0.43	19	1.34	56
G1F3	0.62	18	1.25	59
G1F5	0.63	33	1.07	63
G2F1	0.35	17	1.15	49
G2F3	0.39	7	1.10	47
G2F5	0.46	9	1.00	46
Average	0.48	—	1.15	—

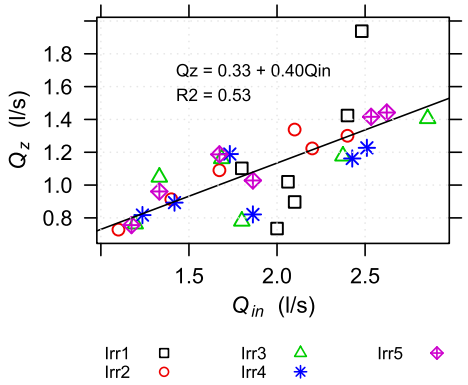

Fig. 9. Furrow near-steady infiltration rate as a function of inflow rate.

procedure. With the exception of the first irrigation, c_{GA} varied systematically from one irrigation to the next [Fig. 8(b)].

Summary statistics calculated for each furrow (Table 8) show that, on average, K_s and c_{GA} values were greater for the furrows in Group 1 than for the furrows in Group 2. This could be the result of textural differences, inflow rate, or both. Clearly, c_{GA} was more variable than K_s throughout the irrigation season, as shown by the COV values.

As noted previously, K_s and $V_{z(sto)}$ values were strongly correlated. A problem with the K_s values is that they were also strongly correlated with Q_{in}. The reasons for this correlation are not clear. One explanation is that, because inflow rates varied systematically among furrows, it is possible that inflow rates were determined based on known differences in infiltration rates among furrows. Another possible explanation is that, under the soil conditions of these tests, lower inflow rates and flow velocities caused greater deposition of sediments and reduced infiltration rates.

The aforementioned WGA parameters were estimated using pedotransfer function–derived values for θ_s and h_f. The potential range of variation for h_f can be expected to be greater than that for θ_s, and the results can be expected to be most sensitive to that parameter. Limited sensitivity tests were conducted with the available data, by varying h_f by $\pm 25\%$. In principle, estimates of c_{GA} depend on crack/macropore flow and are unrelated to h_f. However, h_f could change the amount of water attributed to porous media flow during the early infiltration stages and, therefore, change c_{GA}. For these test, c_{GA} estimates were not affected, which attests to the relative magnitude of macropore flow infiltration at short opportunity times. In contrast, K_s estimates were affected; there was a 17% reduction in K_s when h_f was set to -55.3 cm, and a 25% increase when h_f was set to -32.3 cm. Hence, imprecise values of h_f have a substantial effect on hydraulic conductivity estimates, and the effect is inversely proportional, or nearly so. Imprecise h_f values, however, should not affect the variance of K_s estimates.

Wetted Perimeter Effects on Infiltration

Fig. 9 depicts the furrow infiltration rates as a function of the inflow rate measured close to cutoff time. The data exhibited substantial scatter, especially those from Irrigation 1. Some of the scatter may be attributable to nonsteady state conditions. Nevertheless, the results support the premise that infiltration rate increases with inflow rate, presumably due to a larger wetted perimeter. The equation of the linear regression model, shown in the graph, was statistically significant. The expectation was that this relationship and the theoretical one would share similar slopes.

The simulation analysis produced a well-defined linear relationship between Q_z and Q_{in}. However, the slope of the resulting linear regression model was less than a fifth of that derived from the measured data, $Q_z = 0.99 + 0.072Q_{in}$. Consequently, these results also support the hypothesis that larger inflow rates and, therefore, larger flow velocities, enhance infiltration rates.

Implications for Irrigation System Management and Performance Assessment

Infiltration functions were computed from the estimated WGA parameters. Plots of these functions (Fig. 10) help to further understand the spatial and seasonal variations in intake characteristics for these furrows. The curves were computed for a common flow rate, roughness coefficient, and furrow cross section to eliminate the effect of variable flow conditions among the tests. The results suggest again that the furrows in Group 1 had larger infiltration rates than those in Group 2, even though this factor was eliminated as a predictor by the statistical analysis. The results also show that infiltration rates declined as the irrigation season progressed, except between Irrigations 4 and 5. Again, the short interval between Irrigations 3 and 4 may explain why the lowest infiltration rates are associated, mostly, with Irrigation 4. Note also that the functions developed for Irrigation 1 generally predicted larger infiltration rates than for other events. The exceptions were Furrow 5 in Group 2, for which irrigation 1 produced the lowest infiltration rates, and Furrow 3, Group 2, for which irrigation 3 produced the largest infiltration rates. Infiltration characteristics tend to be most variable early in the irrigation season due to differences in soil consolidation, and this may be a factor that can account for these results. Because this was also the first evaluation of the irrigation season, it is also possible that the results could have been affected by measurement errors.

When conducting a hydraulic analysis of an irrigation system, a key consideration is the opportunity time needed to infiltrate the irrigation requirement depth. The infiltrated depth for the Benson irrigations was generally around 6 cm. The plots in Fig. 10 provide a measure of how infiltration variability complicates the design and management of furrow irrigation systems. For a 6-cm irrigation requirement, the required opportunity time varies between about 5 and 17 h. This variation is largely the result of small differences in the values of K_s, which, as was noted previously, seem to vary consistently for most furrows from one irrigation event to the next.

Despite the large variability, this information can be used to improve the operation of the irrigation system, as will be demonstrated subsequently. An operational strategy (inflow rate and cutoff time) was developed for the Benson furrows based on the 6-cm irrigation requirement. This analysis assumed that infiltration was described by the overall average K_s and c_{GA} parameters. The solution $Q_{in} = 1.5$ L/s and $t_{co} = 960$ was found by trial and error. This solution yields a predicted application efficiency (AE) (the ratio of the volume of infiltrated water stored in the root zone to

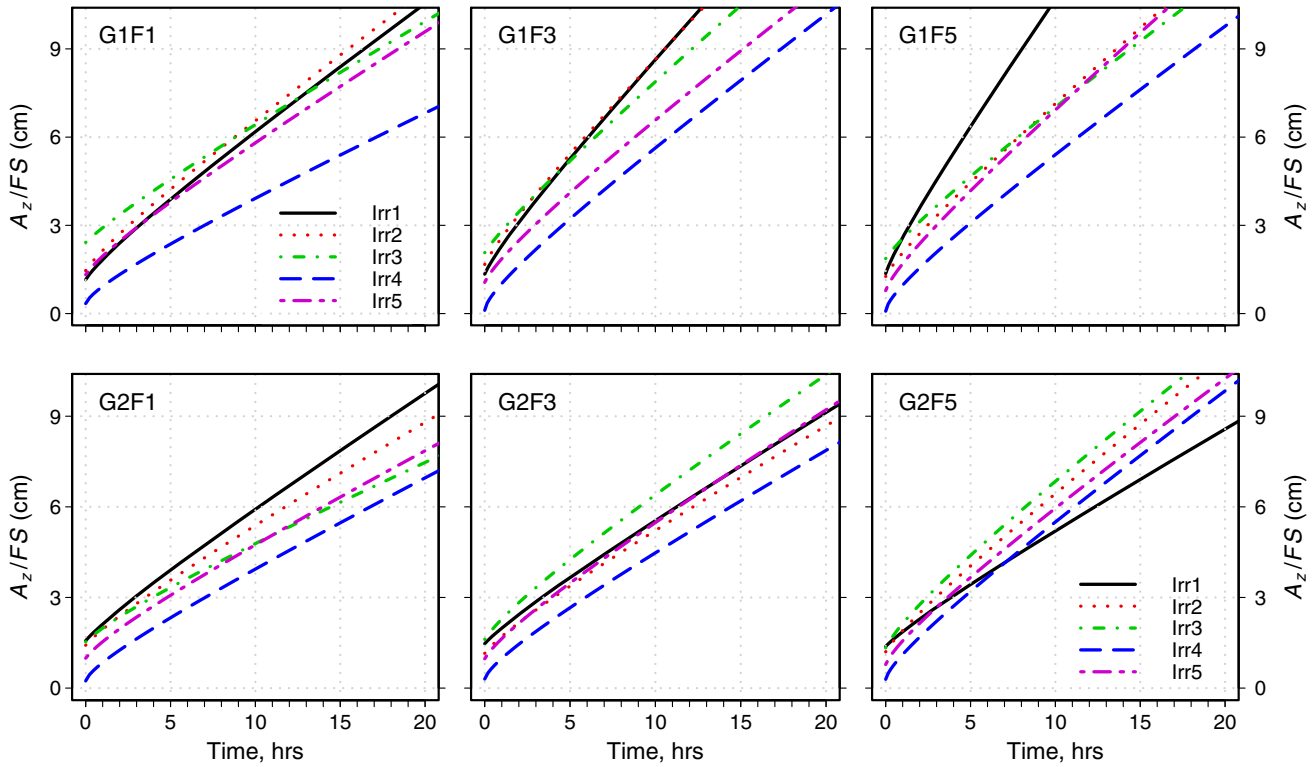

Fig. 10. Estimated WGA infiltration functions computed for each furrow and irrigation using a common inflow rate (2 L/s) and Manning n (0.016). The labels G and F refer to group and furrow numbers, respectively.

the volume applied) of 66% and a requirement efficiency (RE) (the ratio of the volume of infiltrated water stored in the root zone to the volume required to refill the root zone) of 100%. With this operational strategy, nearly half of the losses occur by deep percolation and the rest occur by runoff. In the event that infiltration rates are less than or greater than the rates specified in the analysis, the proposed solution provides some insurance that water will reach the end of the field and that the irrigation requirement will be satisfied for most furrows.

The aforementioned solution was applied to the evaluated furrows using their individually estimated infiltration and resistance parameters. The objective of these simulations was to determine the distribution of AE and RE values, under the assumption that the estimated parameters represent the distribution of infiltration and hydraulic resistance conditions for the field. The average AE from these simulations was 64% with a COV of 6.3%. If the application volume is fixed (by the selected Q_{in} and t_{co} values), then the actual AE can only decline with respect to the design value. RE was better than 95% in 77% of the furrows. Advance failed to reach the end of the field in 10% of the furrows; in one of those cases the resulting RE was 74%, while the other two were better than 90%. Other cases of relatively low RE (85%–95%) were furrows with a low infiltration rate (mostly Irrigation 4), where all water losses were as runoff. The average RE was 97% with a COV of 6.3%. These results can help an irrigator understand differences in performance across an irrigated field, assuming a uniform inflow to all furrows.

Another motivation for using a porous-media flow–based infiltration equation in furrow irrigation modeling is to account for variable wetted perimeter effects along the furrow and represent more realistically the longitudinal distribution of infiltrated water. In principle, the use of empirical infiltration models that do not account for wetted perimeter effects will overestimate infiltration uniformity. The distribution uniformity of the low quarter (DUlq) (Burt et al. 1997) was computed for the 30 evaluations (based on the measured inflow rates) using the modified Kostiakov and WGA infiltration models. As expected, uniformity was always less when computed with the WGA model, but the differences were inconsequential for practical studies—the average difference was less than 0.03. For this data set, shallow flow depths and crack infiltration were factors that contributed to reducing the difference between the DUlq values computed with the two models. Hanson et al. (1998) noted that soil cracking helps to enhance distribution uniformity in furrow systems.

Discussion and Conclusions

The spatial and temporal variability of infiltration in furrow-irrigated fields can be substantial, even when measured on the scale of complete furrows. Several factors that contribute to this variability were examined in this study.

For the particular field conditions, the structure of infiltration variability was different for infiltration measured at the end of the advance phase than for infiltration measured at later times, during the postadvance phase. As demonstrated by the results of Irrigation 4, the volume of water needed to reach the end of the field can vary substantially from one irrigation event to the next. Furthermore, inflow rate differences among furrows had no measurable effect on infiltration variations during advance for any irrigation event. This suggests that the infiltration process was dominated at short opportunity times by crack and/or macropore flow and that the contribution of other factors to infiltration variability was relatively negligible.

A premise of this study was that inflow rate variation contributes to infiltration variability through its effect on wetted perimeter and infiltrating area. This effect may be difficult to establish due to the influence of other factors. Variation in inflow rate among furrows affects advance times and, consequently, the time available for water to infiltrate during the storage phase. The results suggest that furrow infiltration rates increase with inflow rate but not in proportion to changes in wetted perimeter. As indicated previously, it is possible that furrow infiltration rates may be enhanced by larger inflows and flow velocities by preventing sediment deposition. The results also suggest differences in the porous media characteristics of furrows and that these characteristics vary systematically between irrigations, primarily due to soil consolidation and changes in water content.

The proposed WGA equation in combination with the macropore infiltration component modeled furrow infiltration reasonably well and produced smaller values for the estimation objective function than an empirical infiltration equation for the range of soil and hydraulic conditions examined here. While the concept of a volume of water that infiltrates instantaneously seems overly simplistic, such an approach appears to be a practical way of representing the infiltration flow at short times. One potential way to improve the model is to limit macropore infiltration to the available flow rate at a particular location and time, as determined by an unsteady irrigation simulation model.

The estimation procedure produced coherent results for the infiltration and roughness parameters. Hence, as shown by the results in Fig. 8, those parameters show some spatial and temporal structure. Hydraulic conductivities were found to be strongly correlated with V_{zf}, and the values for the macropore constant were correlated to V_{zadv}. The estimated K_s values were of similar magnitude to values reported in the literature. Differences between K_s values computed for different furrows tended to vary systematically during the season, and those values mostly displayed gradual changes for each furrow during the irrigation season. The macroporosity parameter c_{GA} exhibited greater variation than K_s, but mostly between irrigation events and less between furrows for an irrigation event.

This analysis assumes that the macropore term is a function of furrow spacing and that water does not flow between neighboring furrows. The fact that c_{GA} was relatively consistent for an irrigation event suggests that this assumption is largely true. However, the analysis also assumes that water that infiltrates through macropores does not flow past the root zone. Bypass flow is a mechanism that needs to be studied in order to better understand the ultimate irrigation distribution uniformity.

Notation

The following symbols are used in this paper:

AE = application efficiency (%);
A_0 = upstream cross-sectional area;
A_z = infiltration volume per unit length;
c_{GA} = WGA empirical macropore term;
DUlq = distribution uniformity of the low quarter;
FS = furrow spacing;
h_{1D} = wetted-perimeter averaged ponding depth;
h_f = pressure head at the wetting front;
K_s = saturated hydraulic conductivity;
k, a, b, c = parameters of the empirical modified Kostiakov formula for infiltration volume per unit area;
n = Manning roughness coefficient;
Q_{in} = furrow inflow rate;
Q_z = furrow infiltration rate;
RE = requirement efficiency (%);
RMSE = root-mean-square error;
S_0 = soil sorptivity;
SD = standard deviation;
SSQ = sums of squares;
T_{adv} = advance time;
V_{in} = inflow volume;
V_{req} = irrigation requirement volume;
V_{ro} = runoff volume;
V_y = surface volume;
V_z = infiltration volume;
V_{zadv} = infiltration volume at the end of the advance phase;
V_{zf} = infiltration volumes as determined at the final volume balance calculation time, as determined by the particular data;
V_{ziot} = infiltration volume computed for a specified furrow-averaged intake opportunity time;
W = transverse width;
WP = wetted perimeter;
x_A = length of the stream at a given time;
y_0 = flow depth;
z = one-dimensional infiltration volume per unit area;
z_0 = infiltration at time t_0;
γ = empirical parameter related to boundary conditions, geometry, and initial conditions;
$\Delta\theta$ = difference between the saturated and initial water content;
Δh = difference between the average water pressure at the infiltrating surface h_{1D} and the wetting front pressure head h_f;
ε = random error in a multivariable regression analysis;
θ_0, θ_s = initial and saturated volumetric water content; and
σ_y = dimensionless shape parameter for the surface flow.

References

Ahuja, L. R., D. G. Decoursey, B. B. Barnes, and K. W. Rojas. 1993. "Characteristics of macropore transport studied with the ARS root zone water quality model." *Trans. ASAE* 36 (2): 369–380. https://doi.org/10.13031/2013.28348.

Banti, M., T. Zissis, and E. Anastasiadou-Partheniou. 2011. "Furrow irrigation advance simulation using a surface–subsurface interaction model." *J. Irrig. Drain. Eng.* 137 (5): 304–314. https://doi.org/10.1061/(ASCE)IR.1943-4774.0000293.

Bautista, E. 2016. "Effect of infiltration modeling approach on operational solutions for furrow irrigation." *J. Irrig. Drain. Eng.* 142 (12): 06016012. https://doi.org/10.1061/(ASCE)IR.1943-4774.0001090.

Bautista, E., A. J. Clemmens, T. S. Strelkoff, and J. Schlegel. 2009. "Modern analysis of surface irrigation systems with WinSRFR." *Agric. Water Manage.* 96 (7): 1146–1154. https://doi.org/10.1016/j.agwat.2009.03.007.

Bautista, E., and J. L. Schlegel. 2017a. "A flexible system for estimation of infiltration and hydraulic resistance parameters in surface irrigation." *Trans. ASABE* 60 (4): 1223–1234. https://doi.org/10.13031/trans.12117.

Bautista, E., and J. L. Schlegel. 2017b. "Estimation of infiltration and hydraulic resistance in furrow irrigation with infiltration dependent on flow depth." *Trans. ASABE* 60 (6): 1873–1884. https://doi.org/10.13031/trans.12263.

Bautista, E., T. Strelkoff, and A. J. Clemmens. 2012. "Improved surface volume estimates for surface irrigation balance calculations."

J. Irrig. Drain. Eng. 138 (8): 715–726. https://doi.org/10.1061/(ASCE)IR.1943-4774.0000461.

Bautista, E., and W. W. Wallender. 1985. "Spatial variability of infiltration in furrows." *Trans. ASAE* 28 (6): 1846–1851. https://doi.org/10.13031/2013.32529.

Bautista, E., A. W. Warrick, J. L. Schlegel, K. R. Thorp, and D. J. Hunsaker. 2016. "Approximate furrow infiltration model for time-variable ponding depth." *J. Irrig. Drain. Eng.* 142 (11): 04016045. https://doi.org/10.1061/(ASCE)IR.1943-4774.0001057.

Bautista, E., A. W. Warrick, and T. S. Strelkoff. 2014. "New results for an approximate method for calculating two-dimensional furrow infiltration." *J. Irrig. Drain. Eng.* 140 (10): 04014032. https://doi.org/10.1061/(ASCE)IR.1943-4774.0000753.

Burt, C. M., A. J. Clemmens, T. S. Strelkoff, K. H. Solomon, R. D. Bliesner, L. A. Hardy, T. A. Howell, and D. E. Eisenhauer. 1997. "Irrigation performance measures: Efficiency and uniformity." *J. Irrig. Drain. Eng.* 123 (6): 423–442. https://doi.org/10.1061/(ASCE)0733-9437(1997)123:6(423).

Caffo, B. 2015. "Regression models for data science in R." In *A companion book for the Coursera Regression Models class*. Victoria, BC, Canada: Lean Publishing.

Childs, J. L., W. W. Wallender, and J. W. Hopmans. 1993. "Spatial and seasonal variation of furrow infiltration." *J. Irrig. Drain. Eng.* 119 (1): 74–90. https://doi.org/10.1061/(ASCE)0733-9437(1993)119:1(74).

Clemmens, A. J., and E. Bautista. 2009. "Toward physically based estimation of surface irrigation infiltration." *J. Irrig. Drain. Eng.* 135 (5): 588–596. https://doi.org/10.1061/(ASCE)IR.1943-4774.0000092.

Enciso-Medina, J., D. Martin, and D. Eisenhauer. 1998. "Infiltration model for furrow irrigation." *J. Irrig. Drain. Eng.* 124 (2): 73–79. https://doi.org/10.1061/(ASCE)0733-9437(1998)124:2(73).

Fangmeier, D. D., and M. K. Ramsey. 1978. "Intake characteristics of irrigation furrows." *Trans. ASAE* 21 (4): 696–700. https://doi.org/10.13031/2013.35370.

Fonteh, M. F., and T. Podmore. 1993. "A physically based infiltration model for furrow irrigation." *Agric. Water Manage.* 23 (4): 271–284. https://doi.org/10.1016/0378-3774(93)90040-H.

Gillies, M. H., R. J. Smith, and S. R. Raine. 2011. "Evaluating whole field irrigation performance using statistical inference of inter-furrow infiltration variation." *Biosystems Eng.* 110 (2): 134–143. https://doi.org/10.1016/j.biosystemseng.2011.07.008.

Green, W. H., and G. A. Ampt. 1911. "Studies on soil physics. Part 1: The flow of air and water through soils." *J. Agric. Sci.* 4 (1): 1–24. https://doi.org/10.1017/S0021859600001441.

Guzmán-Rojo, D. P. 2017. "Variabilidad de la infiltración y desempeño del riego por surcos, en suelos con características macroporosas." [In Spanish.] M.S. thesis, Dept. of Applied Engineering/Water Resources, Universidad Autónoma de Zacatecas.

Hanson, B. R., A. Fulton, and D. A. Goldhamer. 1998. "Cracks affect infiltration of furrow crop irrigation." *Calif. Agric.* 52 (2): 38–42. https://doi.org/10.3733/ca.v052n02p38.

Hunsaker, D. J., D. A. Bucks, and D. B. Jaynes. 1991. "Irrigation uniformity of level basins as influenced by variations in soil water content and surface elevation." *Agric. Water Manage.* 19 (4): 325–340. https://doi.org/10.1016/0378-3774(91)90025-E.

Izadi, B., and W. W. Wallender. 1985. "Furrow hydraulic characteristics and infiltration." *Trans. ASAE* 28 (6): 1901–1908. https://doi.org/10.13031/2013.32539.

Jaynes, D. B., and D. J. Hunsaker. 1989. "Spatial and temporal variability of water content and infiltration on a flood irrigated field." *Trans. ASAE* 32 (4): 1229–1238. https://doi.org/10.13031/2013.31139.

Khatri, K. L., and R. J. Smith. 2006. "Real-time prediction of soil infiltration characteristics for the management of furrow irrigation." *Irrig. Sci.* 25 (1): 33–43. https://doi.org/10.1007/s00271-006-0032-1.

Mitchell, A. R., and M. T. van Genuchten. 1993. "Flood irrigation of a cracked soil." *Soil Sci. Soc. Am. J.* 57 (2): 490–497. https://doi.org/10.2136/sssaj1993.03615995005700020032x.

Oyonarte, N. A., L. Mateos, and M. J. Palomo. 2002. "Infiltration variability in furrow irrigation." *J. Irrig. Drain. Eng.* 128 (1): 26–33. https://doi.org/10.1061/(ASCE)0733-9437(2002)128:1(26).

Rawls, W. J., D. L. Brakensiek, and N. Miller. 1983. "Green-Ampt infiltration parameters from soils data." *J. Hyd. Eng.* 109 (1): 62–70. https://doi.org/10.1061/(ASCE)0733-9429(1983)109:1(62).

R Core Team. 2017. *R: A language and environment for statistical computing*. Vienna, Austria: R Foundation for Statistical Computing.

Saxton, K. E., and W. J. Rawls. 2006. "Soil water characteristic estimates by texture and organic matter for hydrologic solutions." *Soil Sci. Soc. Am. J.* 70 (5): 1569–1578. https://doi.org/10.2136/sssaj2005.0117.

Šimůnek, J., N. J. Jarvis, M. T. van Genuchten, and A. Gärdenäs. 2003. "Review and comparison of models for describing non-equilibrium and preferential flow and transport in the vadose zone." *J. Hydrol.* 272 (1–4): 14–35. https://doi.org/10.1016/S0022-1694(02)00252-4.

Strelkoff, T. S., A. J. Clemmens, and E. Bautista. 2009. "Estimation of soil and crop hydraulic properties." *J. Irrig. Drain. Eng.* 135 (5): 537–555. https://doi.org/10.1061/(ASCE)IR.1943-4774.0000088.

Tarboton, K. C., and W. W. Wallender. 1989. "Field-wide furrow infiltration variability." *Trans. ASAE* 32 (3): 913–918. https://doi.org/10.13031/2013.31090.

Trout, T. J. 1992a. "Flow velocity and wetted perimeter effects on furrow infiltration." *Trans. ASAE* 35 (3): 855–863. https://doi.org/10.13031/2013.28670.

Trout, T. J. 1992b. "Furrow flow velocity effect on hydraulic roughness." *J. Irrig. Drain. Eng.* 118 (6): 981–987. https://doi.org/10.1061/(ASCE)0733-9437(1992)118:6(981).

Walker, W. R., and B. Kasilingam. 2004. "Another look at wetted perimeter along irrigated furrows—Modeling implications." In *Proc., 2004 World Water and Environmental Research Congress Critical Transitions in Water Environmental Resources Management*, 1664–1670. Reston, VA: ASCE.

Warrick, A. W., N. Lazarovitch, A. Furman, and D. Zerihun. 2007. "Explicit infiltration function for furrows." *J. Irrig. Drain. Eng.* 133 (4): 307–313. https://doi.org/10.1061/(ASCE)0733-9437(2007)133:4(307).

Wöhling, T., and G. H. Schmitz. 2007. "Physically based coupled model for simulating 1D surface–2D subsurface flow and plant water uptake in irrigation furrows. Part I: Model development." *J. Irrig. Drain. Eng.* 133 (6): 538–547. https://doi.org/10.1061/(ASCE)0733-9437(2007)133:6(538).